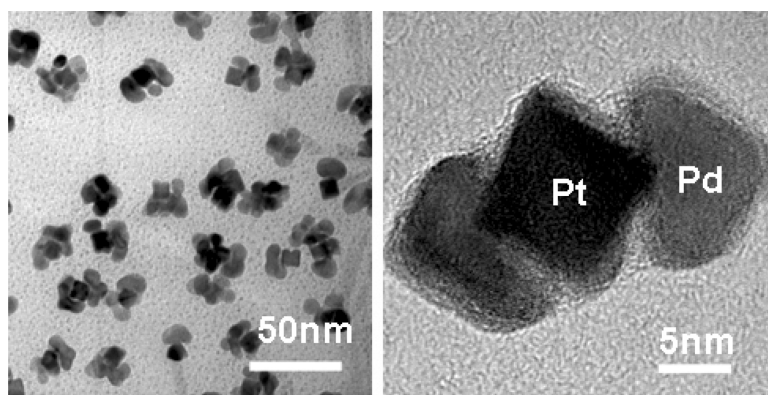


## Localized Pd Overgrowth on Cubic Pt Nanocrystals for Enhanced Electrocatalytic Oxidation of Formic Acid

Hyunjoo Lee, Susan E. Habas, Gabor A. Somorjai, and Peidong Yang

*J. Am. Chem. Soc.*, **2008**, 130 (16), 5406-5407 • DOI: 10.1021/ja800656y • Publication Date (Web): 26 March 2008

Downloaded from <http://pubs.acs.org> on February 8, 2009



### More About This Article

Additional resources and features associated with this article are available within the HTML version:

- Supporting Information
- Links to the 2 articles that cite this article, as of the time of this article download
- Access to high resolution figures
- Links to articles and content related to this article
- Copyright permission to reproduce figures and/or text from this article

[View the Full Text HTML](#)

## Localized Pd Overgrowth on Cubic Pt Nanocrystals for Enhanced Electrocatalytic Oxidation of Formic Acid

Hyunjoon Lee,<sup>†,‡</sup> Susan E. Habas,<sup>‡</sup> Gabor A. Somorjai,<sup>‡</sup> and Peidong Yang<sup>\*,‡</sup>

Department of Chemical Engineering, Yonsei University, Seoul, South Korea, Department of Chemistry, University of California, Berkeley, California 94720, and Materials Sciences Division, Lawrence Berkeley National Laboratory, Berkeley, California 94720

Received January 26, 2008; E-mail: p\_yang@uclink.berkeley.edu

Single crystalline metal surfaces, such as low index (100), (111), and (110) structures, have been studied as idealized platforms for electrocatalytic reactions because the surface atomic arrangement affects the catalytic properties.<sup>1</sup> Secondary metal deposition on these surfaces also alters the catalytic response, often favorably with improvements such as reduced poisoning.<sup>2</sup> On the other hand, electrocatalysts used for practical purposes usually have a size on the order of nanometers. Therefore, linking the knowledge from single crystalline surface studies to nanoparticle catalysts is of enormous importance. Recently, Pt nanoparticles with preferentially oriented surface structures were synthesized as electrocatalysts.<sup>3</sup> Here, we demonstrate the rational design of a binary metallic nanocatalyst based on a shaped nanoparticle seeding concept.

Clavilier et al. studied the electro-oxidation of formic acid for Pd adsorbed on a Pt(100) single crystal surface.<sup>2a</sup> They observed that the presence of adsorbed palladium on Pt(100) decreases self-poisoning and lowers the oxidation potential considerably. Multimetallic nanoparticle catalysts, however, are usually prepared by coprecipitation<sup>4</sup> or electrodeposition,<sup>5</sup> and control over surface structure is not readily achieved. We present here the synthesis of binary Pt/Pd nanoparticles in which Pd decorates the well-defined surface of Pt nanoparticles. Pt nanocubes fully bound by (100) surfaces acted as seeds for overgrowth of Pd. Overgrowth was observed at multiple points on each seed, predominantly at the corners. Electro-oxidation of formic acid performed on these binary Pt/Pd catalysts showed that oxidation occurred at a lower potential with less poisoning, similar to the effects expected from the single crystalline surface study.

Preparation of metal nanoparticles with shape control has often been achieved by controlling growth rates on different facets through interactions with surface-stabilizing agents.<sup>6</sup> However, since the catalytic activity is hindered by these surface-stabilizing agents, preserving the catalytic activity of the metal surface is crucial. In this study, we used tetradecyltrimethylammonium bromide (TTAB) as a surface-stabilizing agent since it has a weak interaction with metal surfaces.<sup>7</sup> The cubic Pt nanoparticles used as seeds were prepared by reducing K<sub>2</sub>PtCl<sub>4</sub> dissolved in aqueous TTAB solution with NaBH<sub>4</sub> as previously reported.<sup>7</sup> A TEM image of the cubic Pt seed particles is shown in Figure S1a. Pd was nucleated on the surface of cubic Pt seeds upon reduction of K<sub>2</sub>PdCl<sub>4</sub> by ascorbic acid in the presence of TTAB (see Supporting Information for details). Figure 1a shows a low magnification TEM image of

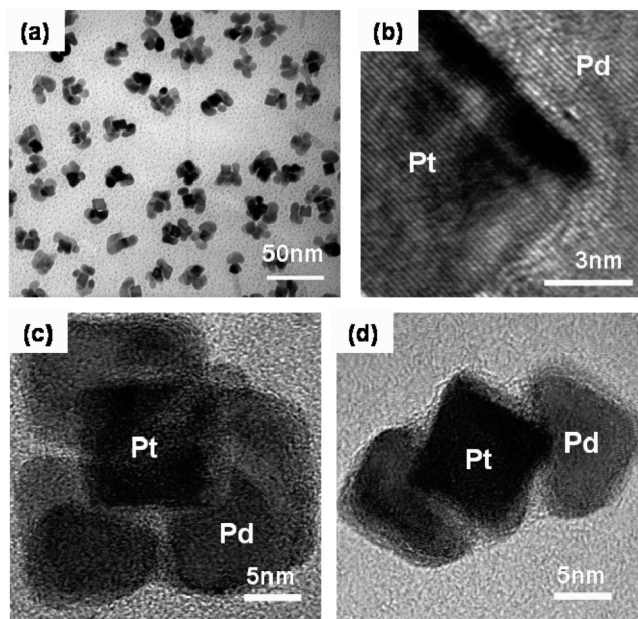


**Figure 1.** TEM images of (a) binary Pt/Pd nanoparticles, HR-TEM images of (b) a Pt/Pd interface, (c) high Pd coverage and (d) low Pd coverage of binary Pt/Pd nanoparticles.

the binary Pt/Pd nanoparticles. Single, double, and multiple nucleation of Pd on a Pt nanoparticle was observed with nucleation occurring primarily on the corners. The high resolution TEM image in Figure 1b shows the interface between the two metals more clearly and also indicates the epitaxial relationship between the Pt and Pd. Figure 1c,d shows examples of high and low coverage of Pd on the Pt surface. The formation of multiple nucleation sites of Pd on the Pt seeds rather than conformal overgrowth depends on the rate of reduction, which was controlled through pH. The addition of as-made Pt seeds (pH ~9) also introduces the strongly basic metaborate ion (BO<sub>2</sub><sup>-</sup>) formed during the reaction of NaBH<sub>4</sub> with water. The higher pH increases the rate of Pd reduction, probably due to better stabilization of the deprotonated form of the ascorbic acid. The increased rate of reduction may encourage the formation of multiple nucleation sites rather than the conformal overgrowth of a thin Pd shell which was observed when the Pt seeds were acidified to a neutral pH.<sup>8</sup> The addition of base to bring the pH of the neutralized seed solution back to ~9 once again allows for the formation of multiple nucleation sites. Pt nanoparticles conformally coated with Pd, shown in Figure S1b, were prepared by decreasing the concentration of Pt seeds along with the pH. This type of epitaxial overgrowth was demonstrated previously.<sup>8</sup>

<sup>†</sup> Yonsei University.

<sup>‡</sup> University of California, Berkeley, and Lawrence Berkeley National Laboratory.

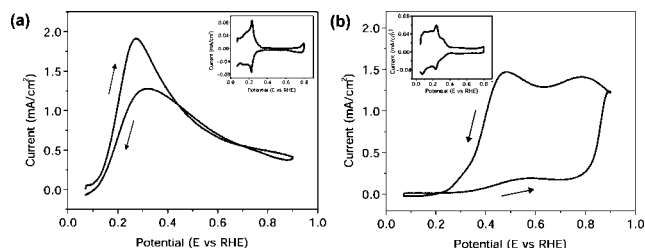


**Figure 2.** Cyclic voltammograms for (a) binary Pt/Pd nanoparticles and (b) Pt nanocubes in 0.25 M HCOOH + 0.5 M H<sub>2</sub>SO<sub>4</sub> solution taken at a scan rate of 50 mV/s. The insets show voltammograms of the same electrodes in 0.5 M H<sub>2</sub>SO<sub>4</sub> at 50 mV/s without formic acid.

While both the Pt and Pd surfaces are accessible on the binary Pt/Pd nanoparticles, only the Pd surface is available on the core-shell Pt/Pd nanocubes. Pd nanoparticles without Pt seeds were also prepared as shown in Figure S1c for comparison.

Each type of nanoparticle, described above, was tested as an electrocatalyst for formic acid oxidation. A washed and concentrated nanoparticle solution was deposited on a Au electrode and dried at room temperature. The presence of the stabilizing agents on the nanoparticle surface required measurement of the actual surface area that was accessible for reaction. The surface areas were estimated from H adsorption/desorption cyclic voltammograms (CV) taken in sulfuric acid solution, and the results for formic acid oxidation were normalized by the estimated surface areas. Clavilier et al. reported that no oxidation was observed in the positive scan for a Pt(100) single crystal surface and a lower oxidation peak potential was observed when Pd was adsorbed on Pt(100) (0.23 V for Pd adsorbed on Pt(100) and 0.42 V for Pt(100)).<sup>2a</sup> The CVs for the nanoparticles were collected under the same electrocatalytic conditions in a solution of 0.25 M HCOOH + 0.5 M H<sub>2</sub>SO<sub>4</sub> at a scan rate of 50 mV/s. Figure 2 shows the CVs for (a) binary Pt/Pd nanoparticles and (b) Pt nanocubes. CVs are provided as insets for the same sample taken in 0.5 M H<sub>2</sub>SO<sub>4</sub> solution without formic acid. CVs for core-shell Pt/Pd nanocubes and Pd nanoparticles synthesized without Pt seed are also shown in Figures S2a,b, respectively. The H adsorption/desorption curves for Pt cubes and Pd cubes correspond well with the CVs for clean (100) surfaces. The blank scan for the binary Pt/Pd nanoparticles is intermediate between those for Pt cubes and Pd cubes, indicating that both the Pt and Pd surfaces are accessible for the reaction.

Formic acid oxidation catalyzed by Pt cubes is strongly hindered by the formation of poisoning intermediates and only minimal oxidation is observed in the positive scan as the case for a single crystal Pt(100) surface.<sup>2a,c</sup> Formic acid oxidation only occurs in the reverse scan after the poison formed in the low potential is oxidized and eliminated from the surface. On the other hand, no inhibition is observed in the positive scan for the binary Pt/Pd nanoparticles. Also, oxidation occurs over a much lower potential range than that observed for Pt cubes (0.27 V for binary Pt/Pd nanoparticles and 0.48 V for Pt cubes). The presence of Pd on the surface of the Pt cubes prevents poisoning in the positive scan and induces a considerable decrease in the activation energy for formic acid oxidation compared with Pt cubes. Formic acid oxidation on Pd cubes and Pd nanoparticles synthesized without Pt seeds was also performed for comparison. In both cases, no inhibition was observed in the positive scan, while the peak oxidation potentials

were as high as or even higher than that for Pt cubes (0.45 V for core-shell Pt/Pd nanocubes and 0.52 V for Pd particles synthesized without Pt seeds).

Pt is known to exhibit a dual path mechanism for the oxidation of formic acid. Direct dehydrogenation produces CO<sub>2</sub> and H<sub>2</sub>, while dehydration produces CO (self-poisoning intermediate) and H<sub>2</sub>O. It has been shown that on Pt the dehydration pathway is predominant at low potential, producing CO.<sup>2d</sup> Voltammetric CO stripping experiments performed on our catalysts show a CO stripping peak that is shifted toward a higher potential for the binary Pt/Pd nanoparticles compared to the Pt cubes (see Figure S3). Although a higher CO stripping potential indicates a lower CO tolerance, binary Pt/Pd nanoparticles show little poisoning in the positive scan. Therefore, the direct dehydrogenation path producing CO<sub>2</sub> and H<sub>2</sub> seems to be followed with Pd overgrowth on the Pt surface, which has also been observed by other research groups.<sup>2d,9</sup> For the binary Pt/Pd nanoparticles, the presence of Pd acts to minimize CO formation at low potential, thus lowering the poisoning and the oxidation peak potential.

Binary Pt/Pd nanoparticles were synthesized by localized overgrowth of Pd on cubic Pt seeds for investigation of electrocatalytic formic acid oxidation. The binary Pt/Pd nanoparticles exhibited much less self-poisoning and a lower activation energy relative to Pt nanocubes, consistent with the single crystalline surface study.

**Acknowledgment.** This work was supported by Office of Basic Energy Sciences, Materials Sciences and Engineering Division, of the U.S. Department of Energy under Contract No. DE-AC02-05CH1123. We thank the National Center for Electron Microscopy for the use of their facilities.

**Supporting Information Available:** Details for synthesis, characterization, and electrocatalytic measurements. Figures S1, S2, and S3. This material is available free of charge via the Internet at <http://pubs.acs.org>.

## References

- (1) (a) Hoshi, N.; Kida, K.; Nakamura, M.; Nakada, M.; Osada, K. *J. Phys. Chem. B* **2006**, *110*, 12480–12484. (b) Karlberg, G. S.; Jaramillo, T. F.; Skulason, E.; Rossmeisl, J.; Bligaard, T.; Norskov, J. K. *Phys. Rev. Lett.* **2007**, *99*, 126101. (c) Motoo, S.; Furuya, N. *J. Electroanal. Chem.* **1985**, *184*, 303–316.
- (2) (a) Llorca, M. J.; Feliu, J. M.; Aldaz, A.; Clavilier, J. *J. Electroanal. Chem.* **1994**, *376*, 151–160. (b) Baldauf, M.; Kolb, D. M. *J. Phys. Chem.* **1996**, *100*, 11375–11381. (c) Vidal-Iglesias, F. J.; Solla-Gullon, J.; Herrero, E.; Aldaz, A.; Feliu, J. M. *J. Appl. Electrochem.* **2006**, *36*, 1207–1214. (d) Arenz, M.; Stamenkovic, V.; Schmidt, T. J.; Wandelt, K.; Ross, P. N.; Markovic, N. M. *Phys. Chem. Chem. Phys.* **2003**, *5*, 4242–4251.
- (3) (a) Solla-Gullon, J.; Vidal-Iglesias, F. J.; Rodriguez, P.; Herrero, E.; Feliu, J. M.; Clavilier, J.; Aldaz, A. *J. Phys. Chem. B* **2004**, *108*, 13573–13575. (b) Tian, N.; Zhou, Z. Y.; Sun, S. G.; Ding, Y.; Wang, Z. L. *Science* **2007**, *316*, 732–735. (c) Wang, C.; Daimon, H.; Kim, J.; Sun, S. *J. Am. Chem. Soc.* **2007**, *129*, 6974–6975.
- (4) (a) Chen, W.; Kim, J.; Sun, S.; Chen, S. *Phys. Chem. Chem. Phys.* **2006**, *8*, 2779–2786. (b) Ye, H.; Crooks, R. M. *J. Am. Chem. Soc.* **2007**, *129*, 3627–3633.
- (5) Jayashree, R. S.; Spindelov, J. S.; Yeom, J.; Rastogi, C.; Shannon, M. A.; Kenis, P. J. A. *Electrochim. Acta* **2005**, *50*, 4674–4682.
- (6) (a) Chen, J.; Herricks, T.; Xia, Y. *Angew. Chem., Int. Ed.* **2005**, *44*, 2589–2592. (b) Teng, X.; Yang, H. *Nano Lett.* **2005**, *5*, 885–891.
- (7) Lee, H.; Habas, S. E.; Kweskin, S.; Butcher, D.; Somorjai, G. A.; Yang, P. *Angew. Chem., Int. Ed.* **2006**, *45*, 7824–7828.
- (8) Habas, S. E.; Lee, H.; Radmilovic, V.; Somorjai, G. A.; Yang, P. *Nat. Mater.* **2007**, *6*, 692–697.
- (9) Babu, P. K.; Kim, H. S.; Chung, J. H.; Oldfield, E.; Wieckowski, A. *J. Phys. Chem. B* **2004**, *108*, 20228–20232.

JA800656Y